Article

Aerodynamics from Cursorial Running to Aerial Gliding for Avian Flight Evolution

Farzeen Shahid [1]**, Jingshan Zhao** [1,]***and Pascal Godefroit** [2]

[1]   State Key Laboratory of Tribology, Department of Mechanical Engineering, Tsinghua University, Beijing 100084, China.; feiz17@mails.tsinghua.edu.cn

[2]   Royal Belgian Institute of Natural Sciences, Vautier street 29, 1000 Brussels, Belgium; Pascal.Godefroit@naturalsciences.be

*   Correspondence: jingshanzhao@mail.tsinghua.edu.cn

check for updates

Abstract: Among the different models that have been proposed to explain the origin of avian flight from terrestrial predators, the cursorial and arboreal hypotheses remain the most discussed. However, the fossil data at hand show that, taken separately, both theories have significant limitations in explaining the origin of flight in bird lineage. Here, we describe an aerodynamics principle that fills in the gaps between those apparently contradictory models. The upslope wind in mountain areas and strong wind in plains provided the meteorological conditions allowing feathered paravians to glide. The results suggest that smaller, feathered paravians could be lifted to glide down to trees on mountain slopes or even to glide up to high trees in plain areas when meeting a strong airflow as they were pursuing a prey or escaping from a predator. The development of more aerodynamical limb feathers was a key factor for gliding down the trees because of the dependency of the resultant force on the surface area of a paravian's body. Later in the evolution process, paravians learned to change the orientation of their wings to gain higher lifts. The proposed principle and the results obtained in the present research help to better estimate the aerodynamic behavior of extinct species and will also help to design an efficient and beneficial system for future flying robots.

Keywords: avian flight; cursorial running; arboreal gliding; aerodynamics; *Anchiornis huxleyi*; evolution

1. Introduction

In modern science, researchers take inspiration from living organisms, such as birds, bats, insects, fishes, etc., and incorporate their behavior into artificial yet useful products. Bio-inspired Micro Aerial Vehicle (MAV) and bionic robots open up a vast and boundless area of research, which is beneficial for industries, commercial companies, and academic institutions. It is a difficult task to mimic the extraordinary amount of maneuverability of flying animals, but by doing so, we can also have an estimate of their aerodynamic performances and biological adaptations [1]. In flying animals, wings are one of the most important anatomical features, because control, power, and flight forces are generated by their motion [2]. In modern birds, layers of feathers over the wing [3] provide different functions during flight, but these feathers passed through an evolutionary process to reach their current structured stage [4]. Recent discoveries of feathered and winged dinosaurs [5] have shed new light on the evolution and origin of flight in bird lineage.

Since the discovery of *Archaeopteryx* in Germany in 1861, the origin of flight in birds has caused fierce debate among paleontologists [6–10]. It is now widely accepted that birds are closely related to paravian theropods, a clade of small, carnivorous dinosaurs that also include *Dromaeosauridae* and *Troodontidae* [10]. Since the discovery of *Sinosauropteryx* in 1998 [11], Late Jurassic and Early

Cretaceous formations in northeastern China have yielded numerous exquisitely preserved fossils of feathered dinosaurs that document the cumulative evolution of avian characters along the theropod lineage [12–16]. It has also been shown that the theropod lineage, which is directly ancestral to birds, underwent sustained miniaturization over 50 million years and evolved skeletal adaptations four times faster than other dinosaurs. After two decades of discoveries, feathers and feather-related structures are known to be widespread among dinosaurs, with more than 50 non-avialan paravian taxa, known from a series of fossils with great ranges of size, osteology, limb proportions, and integumentary covering [4,10]. Although the plumage was not developed for flight initially [5,10,17–20], the feather subsequently provided aerodynamic capabilities for gliding and flapping flights [12,16].

Nevertheless, there is still an intriguing question about how paravian dinosaurs learned to fly [5,8,9]. Traditionally, paleontologists have advanced two theories for explaining the origin of avian flight. The arboreal model, proposed by Marsh in 1880 [7], holds that flight developed in a climbing, tree-dwelling ancestor that was built for gliding but started flapping to extend its aerial time [7,12,20,21]. *Archaeopteryx* possessed the same claw curvature of the foot as that of perching birds, suggesting arboreal habits for this ancestral bird [22–24]. However, evidence for trunk-climbing in *Archaeopteryx* and basal birds is still weak, and the arboreal model is far from being unanimously accepted [6,15]

According to the competing cursorial model, originally outlined by Williston in 1879, flight arose in small, bipedal, terrestrial theropod dinosaurs that sped along the ground with arms outstretched and leapt into the air while pursuing prey or evading predators. Feathers on their forelimbs enhanced the lift, thereby allowing the creatures to take flight [6,7,12]. However, long leg feathers were developed in a series of basal paravians and birds and were obviously an obstacle for speeding up to glide or fly [16,21,25]. In addition, the flight muscles of *Archaeopteryx* only represented 9% of the body mass [26], which is far less than the average 25% of the body mass found in modern birds [27]; hence, *Archaeopteryx* likely had a particularly short and ineffective flapping flight, and, because of its higher mass, *Archaeopteryx* would have to run much faster than modern birds to achieve lift-off.

The wing-assisted incline running (WAIR) hypothesis is a derived version of the cursorial model prompted by observations of chukar chicks; it proposes that wings developed their aerodynamic functions as a result of the need to run quickly up very steep slopes, such as tree trunks, to escape from predators. The progression from wing-assisted incline running to flight can be seen in the growth of birds, from when they are hatchlings to fully grown adults [18].

This article is divided into the following sections: Section 2 describes the environmental conditions that prevailed in northeastern China during the Late Jurassic and Early Cretaceous period, along with the mechanisms of upslope and downslope winds. A vector diagram depicting the instantaneous and relative velocities of airflow and basic aerodynamics in *Anchiornis* is introduced in Section 3. In Section 4, calculations for lift and drag coefficients and the mass and size of ancestral bird are presented. The results of the trajectories of *Anchiornis,* arboreal gliding evolution, and stability control during gliding are discussed in Section 5. Finally, the article is concluded in Section 6.

2. Paleoenvironment of the Earliest Feathered Paravian Dinosaurs

The Jurassic and Early Cretaceous era was a period of intense tectonic movements in eastern Asia. The most important event, known as the "Yanshan movement", affected the northern margin of the North China Craton and was characterized by intensive tectonic deformation and extensive magmatism. The initial Yanshan movement began during the Bathonian (Middle Jurassic), and its main phase took place in the Late Jurassic; the initiation point of this main phase is, for example, recorded in unconformities below the volcanic rocks of the Tiaojishan Formation in northern Hebei Province [28]. Volcanic activity was also intense in the area, as revealed by the abundance of intermediate-basic volcanic deposits, such as andesite, andesitic basal, basaltic andesite, and trachyandesite throughout the sequence. The Tiaojishan flora was dominated by Bennettitales, ferns, and Nilssoniales, followed by ginkgophytes; the floristic signature indicates a subtropical-to-temperate warm and humid climate,

with a consistent and distinct seasonal pattern [29]. In general, the vertebrate fauna of the Tiaojishan Formation are typically preserved in fine-grain lacustrine beds [30].

Chinese *Anchiornithids*, therefore, lived in a particularly rugged environment, including mountains and volcanos, under a warm, humid climate. Such mountain environments are characterized by frequent upslope winds, from valleys to the top of the mountains along the mountainside (Figure 1a), in the daytime and downslope winds (Figure 1b) at night [31–33]. The natural upslope wind in the daytime allowed the theropods to move from the ground to the tall trees on the mountainside. In normal conditions, the maximum speed of the upslope wind varies between 1 and 12 m/s [31,32], with significant seasonal variations [33]. When a strong wind occurs in summer, the speed of the airflow frequently reaches 45 m/s [34]. There is no reason to believe that the natural meteorological rules observed in today's world are not applicable to the Jurassic world.
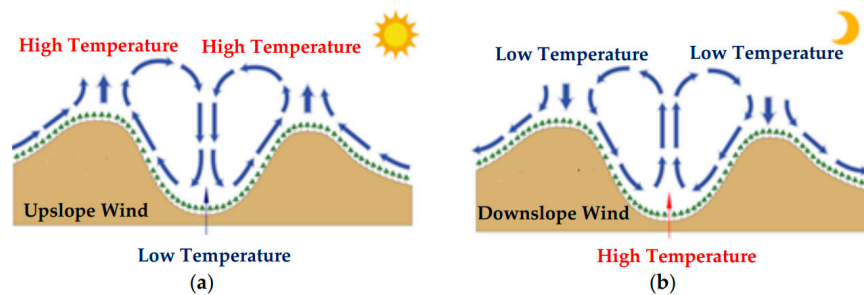

Figure 1. Mechanism of wind: (**a**) upslope; (**b**) downslope.

3. Gliding Aerodynamics in Basal Paravian Dinosaurs

A terrestrial basal paravian theropod, *Anchiornis*, running to capture a prey or to escape from a predator on the top of a mountain, had an initial absolute velocity v_t, which was high enough to be its capacity of running when it encountered an upslope airflow, the velocity of which was v_2 at the brim of the summit of the mountain. The relative velocity of the upslope airflow with respect to the *Anchiornis* v should be the resultant velocity of v_t and v_2, mathematically written as follows:

$$v = v_2 - v_t \tag{1}$$

A balance of projected lift and drag on an *Anchiornis* body is shown in Figure 2a, and its weight is determined by the effective projection area of its body in the equivalent cord EF. The velocity diagram is separately shown in Figure 2b, where the initial absolute velocity v_t is divided into the horizontal and vertical components, v_x and v_y, respectively, and θ is the slope angle of the mountainside.
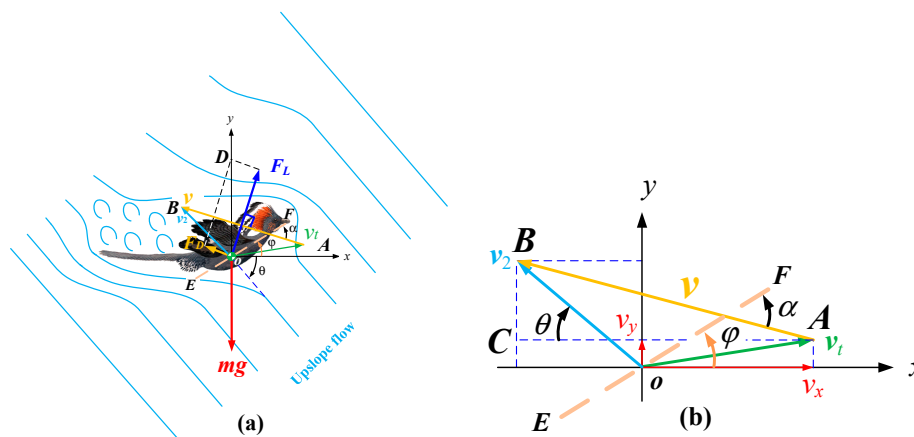

Figure 2. An *Anchiornis* body with (**a**) a balance of projected lift and drag; (**b**) velocity diagram containing the relative airflow.

The magnitude of the relative velocity can be obtained in line with the cosine law of triangle,

$$v = \sqrt{(v_x + v_2 cos\theta)^2 + (v_2 sin\theta - v_y)^2}. \tag{2}$$

According to the sine law of triangle,

$$\angle BAC = \arctan\left(\frac{v_2 sin\theta - v_y}{v_2 cos\theta - v_x}\right). \tag{3}$$

The angle of attack (α) between the equivalent chord EF and the relative velocity v is given below,

$$\alpha = \varphi + \angle BAC = \varphi + \arctan\left(\frac{v_2 sin\theta - v_y}{v_2 cos\theta - v_x}\right). \tag{4}$$

In accordance with the aerodynamics theory, we obtain the following:

$$\left\{ \begin{array}{l} F_L = \frac{1}{2}C_L\rho sv^2 = \frac{1}{2} C_L\rho s\left[(v_x + v_2 cos\theta)^2 + (v_2 sin\theta - v_y)^2\right] \\ F_D = \frac{1}{2} C_D\rho sv^2 = \frac{1}{2} C_D\rho s\left[(v_x + v_2 cos\theta)^2 + (v_2 sin\theta - v_y)^2\right] \end{array} \right\} \tag{5}$$

where F_L represents the magnitude of lift, which is perpendicular to the relative velocity v, and F_D represents the magnitude of drag, which is along the relative velocity v, as illustrated in Figure 2b. Both F_L and F_D result from the aerodynamics of airflow; C_L and C_D are the lift and drag coefficients of *Anchiornis*, which are all the functions of the angle of attack as expressed in Equation (4); ρ is the density of airflow; and s is the effective area of *Anchiornis*.

Therefore, the resultant force exerted on *Anchiornis* of mass m is given by Equation (6), and the trajectory of *Anchiornis* is determined by the resultant forces in vertical and horizontal directions when it leaves the ground. The dynamics differential equations for *Anchiornis* can be obtained from Equation (6) and are presented by Equation (7):

$$\left. \begin{array}{l} R = \left[\begin{array}{c} R_x\left(v_x, v_y, v_2\right) \\ R_y\left(v_x, v_y, v_2\right) \end{array} \right] \\ R = \left[\begin{array}{c} F_L sin\angle BAC - F_D cos\angle BAC \\ F_L cos\angle BAC + F_D sin\angle BAC - mg \end{array} \right] \\ R = \left[\begin{array}{c} \left(\begin{array}{c} \frac{1}{2}\rho s\sqrt{(v_x + v_2 cos\theta)^2 + (v_2 sin\theta - v_y)^2} \\ (v_2 C_L sin\theta - C_L v_y - C_D v_x - C_D v_2 cos\theta) \end{array} \right) \\ \left(\begin{array}{c} \frac{1}{2}\rho s\sqrt{(v_x + v_2 cos\theta)^2 + (v_2 sin\theta - v_y)^2} \\ (C_L v_x + C_L v_2 cos\theta + v_2 C_D cos\theta - C_D v_y) - mg \end{array} \right) \end{array} \right] \end{array} \right\} \tag{6}$$

$$\left. \begin{array}{l} m\frac{d^2x}{dt^2} - \frac{\rho s}{2}\sqrt{(v_x + v_2 cos\theta)^2 + (v_2 sin\theta - v_y)^2} \\ (v_2 C_L sin\theta - C_L v_y - C_D v_x - C_D v_2 cos\theta) = 0 \\ m\frac{d^2y}{dt^2} - \frac{\rho s}{2}\sqrt{(v_x + v_2 cos\theta)^2 + (v_2 sin\theta - v_y)^2} \\ (C_L v_x + C_L v_2 cos\theta + v_2 C_D cos\theta - C_D v_y) - mg = 0 \end{array} \right\} \tag{7}$$

where $\frac{d^2x}{dt^2}$ and $\frac{d^2y}{dt^2}$ represent the accelerations of *Anchiornis* in the horizontal and vertical directions, respectively, and $v_x = \frac{dx}{dt} = v_1$, $v_y = \frac{dy}{dt} = 0$ when $t = 0$. The vertical and horizontal components of the resultant forces are affected by the relative velocity v, the inclined angle of the mountain's slope θ, and the coefficient of lift and drag C_L and C_D. The displacements of *Anchiornis* in the horizontal and vertical directions at any moment are the functions of the animal's initial speed v_t, the airflow speed v_2, and the inclined angle of the mountain slope θ. If *Anchiornis* is gliding towards a perching point at the top of a tree, h is the height from the perching point to the root of the tree. We can analyze its

minimum speed distribution with respect to the airflow speed v_2 and the tilt angle θ of the slope of the mountain by the numerical solutions for Equation (7).

When the inclined angle of the mountain slope θ is specified, the accelerations of *Anchiornis* in the horizontal and vertical directions have determinate distributions with respect to v_2 and v_2, as the lift coefficient C_L and drag coefficient C_D of the wing could be adjusted to have the best ratio of lift over drag, the formulas of which were interpolated from the simulation for the thin flat plate through the fluent software (more detail is presented in the Section 4).

4. Materials and Methods

4.1. Lift and Drag Coefficients

Any shaped object with an angle of attack moving through a fluid will generate an aerodynamic force, the perpendicular component to the motion is called lift, while the parallel component to the moving direction is called drag. Both the lift and drag on the moving body are the primary results of its angle of attack and shape. As the feathers of *Anchiornis* were still primitive, slender and weak [35,36], therefore, its wings might not have the most efficient lifting shapes, as shown in Figure S1(a). We used the most primitive airfoil, a thin flat plate, illustrated in Figure S1(b), with an angle of attack to replace its stretched wing.

For the specified thin flat plate, the lift coefficient and drag coefficient are all the functions of the angle of attack. So, we supposed that the relationship between the angle of attack and the lift and drag coefficients are as follows:

$$\begin{cases} C_L = x_0 + x_1\alpha + x_2\alpha^2 + \ldots + x_n\alpha^n \\ C_D = y_0 + y_1\alpha + y_2\alpha^2 + \ldots + y_n\alpha^n \end{cases} \tag{8}$$

where C_L is the lift coefficient, C_D is the drag coefficient, α is the angle of attack in radian, and x_1 and y_1 (i = 0, 1, 2, $\ldots$, n) are the coefficients of the angle of attack to be determined via simulations.

To get the coefficients of lift and drag of the thin flat plate, we ran the simulation program in fluent software with different angles of attack. The simulation started from 0° to 88°, with an increment of 2° for each step. Substituting the simulation results into Equation (4), we obtained the relationship between the lift coefficient, drag coefficient, and ratio and angle of attack.

$$C_L = 0.053564912 + 1.6115306\alpha - 1.0790198\alpha^2$$

$$C_D = -1.0077079 + 2.1219473\alpha - 0.20780579\alpha^2 + 0.077390225\alpha^3$$

$$\frac{C_L}{C_D} = 0.070129975 + 46.01297\alpha - 246.18671\alpha^2 + 579.0272\alpha^3 - 733.19925\alpha^4 + \tag{9}$$

$$518.02613\alpha^5 - 192.46611\alpha^6 + 29.323193\alpha^7.$$

With the simulation data, we drew C_L, C_D and $\frac{C_L}{C_D}$ through MATLAB, as represented in Figure S2. Using the least square method, we gained their individual interpolated curves to fit these 3 groups of points.

4.2. Mass and Size Parameters of the Ancestors of the Bird

The acceleration of gravity and density were selected from the engineering toolbox. The mass of different dinosaurs were obtained from published paleontological data. The calculation of the areas of the equivalent plate wings were performed as follows. First, we set up the three-dimensional (3D) models of the dinosaurs according to the parameters of the fossils in SolidWorks. Then, we measured the areas of the wings and legs, respectively. The surface area, A, is the sum of the 2 forelimb wings and hind limb wings. Taking *Microraptor* as an example (*Microraptor gui* (IVPP V13352)) [21], the length of the scale bar is 5 cm, which is the reconstruction of *M. gui* showing the morphology and distribution

of the pennaceous feathers. The length of the scale bar is 6 cm. Then, we constructed the 3D model of the dinosaurs according to these materials. We drew the sketch of the wing and the leg and then stretched the sketch in SolidWorks. Finally, we utilized the measuring tools of SolidWorks to get the areas of the wing and leg. The areas of the wings and the legs are 44035.122 mm^2 and 33632.919 mm^2, respectively. As the surface area mainly consists of 2 wings and 2 legs, the total area of the equivalent plate wing equals:

$$A = 2 \times (44035.122 + 33632.919) = 155336.082 \ mm^2.$$

For the point particle model of *Anchiornis huxleyi*, the differential equations for the gliding motion were solved using the well-known Runge–Kutta method. According to the physical theory of momentum, the lift, the drag of the airflow, and the self-weight in gliding were taken into the balance equation of flight in the air. For a multi-point particle system, we use the Newton–Euler method to establish their dynamics equations. Both the forward and inverse solutions could be discussed for the trajectory control of the ancestors of the bird in agile gliding.

5. Results and Discussion

5.1. Trajectories of a Basal Paravian Dinosaur from Cursorial Running to Aerial Gliding

By substituting the mass and size parameters of *Anchiornis* [36] into Equation (7), we can analyze its displacement and trajectory. Assuming that the initial velocity in the horizontal direction was 5 m/s and the inclined angle of the mountainside was θ = 30°, we obtained the trajectories of *Anchiornis*, as shown in Figure 3a, as v_2 changed from 0 to 12 m/s. When the speed of the upslope wind changed from 0 m/s to 6 m/s within this velocity range of airflow, there was almost no possibility for the creature to glide up to a tree on the mountain slope, as shown in Figure 3b. When the speed of the upslope wind changed from 8 to 12 m/s within this velocity range of airflow, the creature could glide up to the branch of a tree of 6-m height when its horizontal displacement was about 15 m on the mountainside, as shown in Figure 3c. The detailed calculation for different velocities is illustrated in Figures S3–S5.
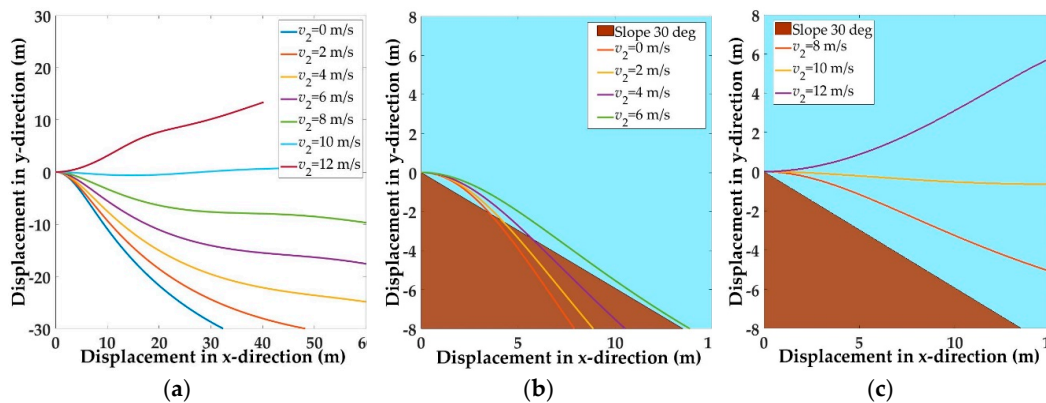

Figure 3. Trajectories of *Anchiornis* running at a speed of 5 m/s and θ = 30°: (**a**) v_2 changes from 0 to 12 m/s; (**b**) v_2 changes from 0 to 6 m/s; (**c**) v_2 changed from 8 to 12 m/s.

Now, assuming that the initial velocity in the horizontal direction was 5 m/s and the inclined angle was θ = 10°, we obtained the trajectories of *Anchiornis*, as shown in Figure 4a, as v_2 changed from 0 to 12 m/s. When the speed of the upslope wind changed from 0 to 6 m/s within the velocity range of airflow, the creature could barely glide on the mountainside, as shown in Figure 4b. When the speed of the upslope wind changed from 8 to 12 m/s within this velocity range of airflow, the creature could glide up to a tree branch higher than 1.2 m when its horizontal displacement was about 8–9 meters on the mountainside, as represented by Figure 4c. The detailed calculation for different velocities is illustrated in Figures S6–S8.
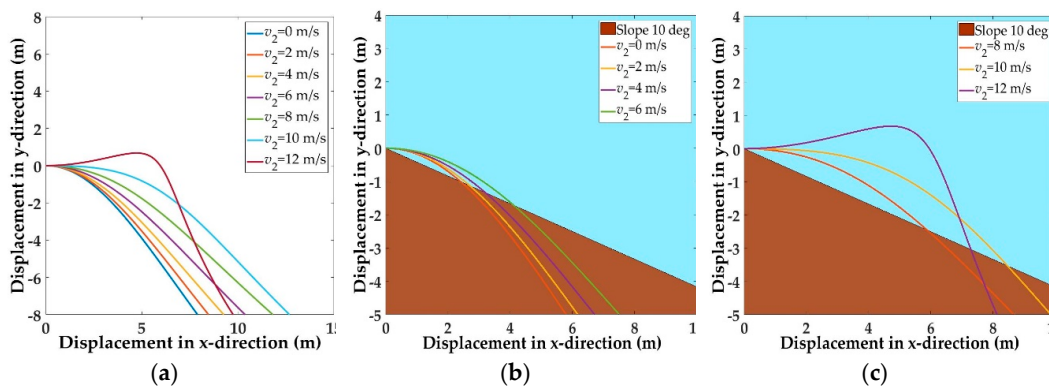
Figure 4. Trajectories of *Anchiornis* running at a speed of 5 m/s and $\theta = 10°$: (**a**) v_2 changes from 0 to 12 m/s; (**b**) v_2 changes from 0 to 6 m/s; (**c**) v_2 changes from 8 to 12 m/s.

Now, assuming that the initial velocity in the horizontal direction was 5 m/s and the inclined angle was $\theta = 0°$, which corresponded to the case on the plain ground, we obtained the trajectories of *Anchiornis*, as shown in Figure 5a, as v_2 changed from 0 to 12 m/s. When the speed of the wind changed from 0 to 12 m/s within this velocity range of airflow, there was no possibility for the creature to glide up to any tree, as shown in Figure 5b. The detailed calculation for different velocities is illustrated in Figures S9–S10.
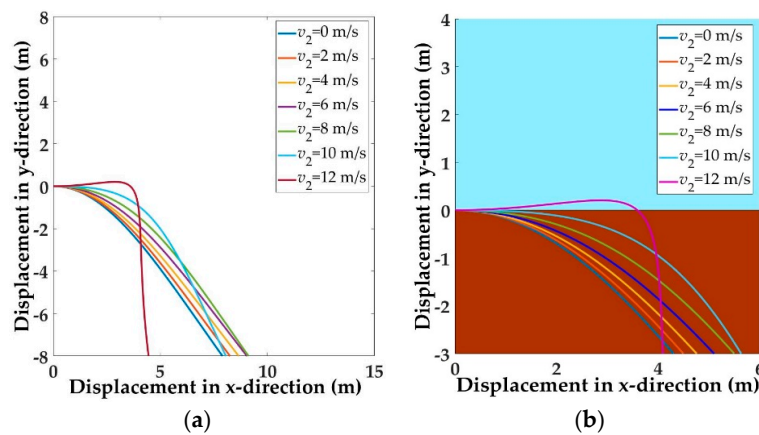

Figure 5. Trajectories of *Anchiornis* running at a speed of 5 m/s and $\theta = 0°$: (**a**) v_2 changes from 0 to 12 m/s; (**b**) v_2 changes from 0 to 12 m/s.

Assuming that the initial velocity in the horizontal direction was 8 m/s and the inclined angle was $\theta = 0°$, which corresponded to the case on the plain ground, we obtained the trajectories, as shown in Figure 6a for *Anchiornis*, as v_2 changed from 0 to 12 m/s. When the speed of the wind changed from 0 to 6 m/s within this velocity range of airflow, there was no possibility for *Anchiornis* to glide up to any tree, as shown in Figure 6b. When the speed of the wind changed from 8 to 12 m/s within this velocity range of airflow, there was the possibility for *Anchiornis* to glide up to 3 m.

The above analysis is based on *Anchiornis*; therefore, similar conclusions can be drawn when we consider the mass parameters of other paravian dinosaurs, including *Epidexipteryx* [37], *Microraptor* [38], *Archaeopteryx* [39], and *Confuciusornis* [40], as summarized in Table 1. These dinosaurs are within the range from 0.11 kg to 1.5 kg, and the effective area parameters are within the range from 0.0132 m^2 to 0.0496 m^2. Substituting the possible mass and size parameters of dinosaurs from Table 1 into Equation (7), we can draw the conclusions that when the running speed of a cursorial dinosaur was from 5 to 8 m/s and the tilt angle of the mountainside θ was larger than 0° but less than 30°, the dinosaur could be lifted to follow a certain trajectory, falling into an interval that covered a tree on the mountainside.
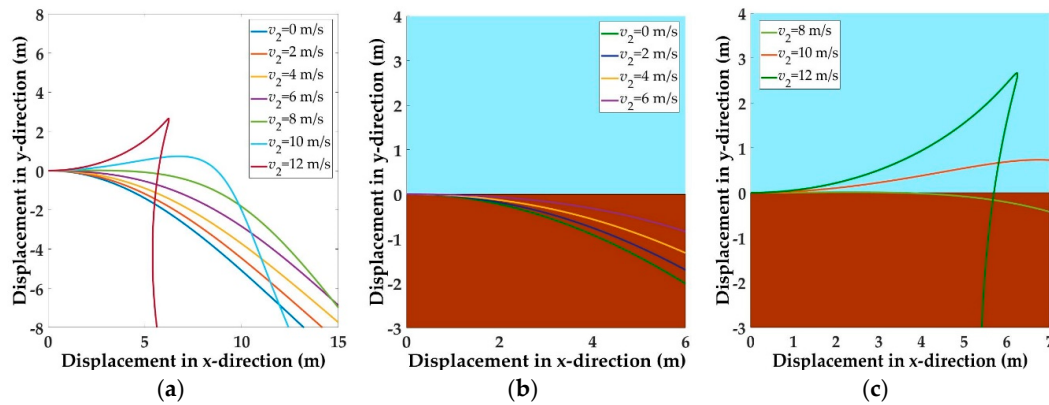
Figure 6. Trajectories of *Anchiornis* running at a speed of 8 m/s and $\theta = 0°$: (**a**) v_2 changes from 0 to 12 m/s; (**b**) v_2 changes from 0 to 6 m/s; (**b**) v_2 changes from 8 to 12 m/s.

Table 1. Living era, mass, effective area, and fossil pictures of *Epidexipteryx*, *Anchiornis*, *Archaeopteryx*, *Microraptor*, and *Confuciusornis*.

Species	Date (m. years)	Mass, *m* (Kg)	Area, A (m²)	Figure of Fossil
Epidexipteryx	152–168 [37]	0.164 [37]	0.0132 [37]	[37]
Anchiornis	155 [36]	0.110 [37]	0.04212 [36]	[36]
Archaeopteryx	150 [38]	0.276 [40]	0.0496 [41]	[41]
Microraptor	110–120 [42]	1.50 [43]	0.155 [21]	[21]
Confuciusornis	120 [40]	0.500 [40]	0.0402 [40]	[40]

Theoretical analysis indicates that the meteorological conditions in the mountain and plain areas allowed the theropods to move from ground to trees. From the viewpoint of taking off from the ground, the velocity threshold is much lower than those predicted earlier [22]. Equation (6) indicates that the vertical component of the resultant force exerted on the dinosaur was dependent on the surface area of the body plane. Therefore, the longer and stronger the feather, the larger the area and the vertical component of the resultant force. So, glide activity propelled the development of the feathers of the bird's ancestors. The early ancestors of the bird could develop longer and longer feathers to adapt to the need for gliding activities. Therefore, the terrestrial theropods could easily benefit from the action of upslope winds in mountain areas or strong winds in plain grounds to get to the trees from the ground and again glide back to the ground.

After calculating the speed of the upslope wind for different cases when the dinosaur was running at a speed from 5 to 8 m/s and the inclined angle θ varied from 30° to 0° (Table 2), we obtained all the possible trajectories of *Epidexipteryx* and *Anchiornis* from ground to air. The trajectories of *Anchiornis* were obtained for three cases when *Anchiornis* was running at a speed of 5 m/s. Assuming that there is a tree at a distance of 10 m along x-direction, the value of v_2 changes from 0 to 7.75 m/s, 7.75 to 9.35 m/s, and 9.35 to 11.20 m/s, for case 1, case 2, and case 3, respectively, as shown in Figure 7a. Similarly, the trajectories at a speed of 8 m/s can be obtained for *Anchiornis* when v_2 changes from 0 to 2.71 m/s, 2.71 to 5.85 m/s, and 5.85 to 9.83 m/s, respectively, for case 1, case 2, and case 3, as shown in Figure 7b. The same analysis is performed on *Epidexipteryx* for all three cases at the speeds 5 m/s and 8 m/s, as shown in Figure 7c,d, respectively.

Table 2. The speed of the upslope wind in different cases when the species ran at the speeds of 5 m/s and 8 m/s and the inclined angle was $\theta = 30°$.

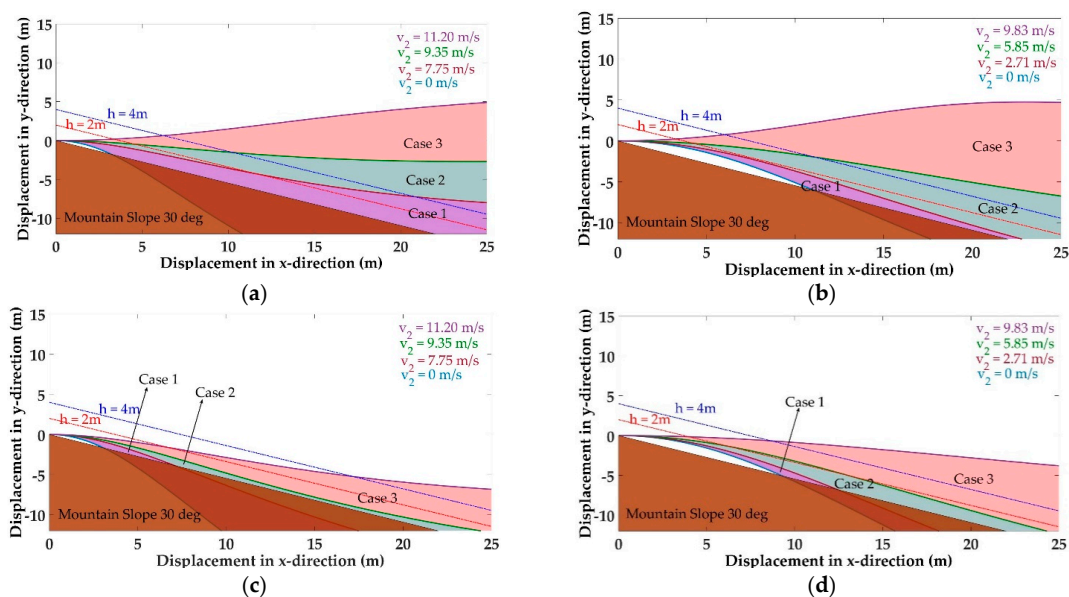| Species	$v_1(\frac{m}{s})$	*Case* 1 $v_2(\frac{m}{s})$	*Case* 2 $v_2(\frac{m}{s})$	*Case* 3 $v_2(\frac{m}{s})$
Epidexipteryx	5	0–7.75	7.75–9.35	9.35–11.20
Anchiornis	5	0–7.75	7.75–9.35	9.35–11.20
Epidexipteryx	8	0–2.71	2.71–5.85	5.85–9.83
Anchiornis	8	0–2.71	2.71–5.85	5.85–9.83

Figure 7. Trajectories of *Anchiornis* running at a speed of: (**a**) 5 m/s; and (**b**) 8 m/s; Trajectories of *Epidexipteryx* running at a speed of: (**c**) 5 m/s; and (**d**) 8 m/s.

5.2. Evolution of Arboreal Gliding

In the course of their evolution, paravian dinosaurs and early birds progressively developed longer, stiffer, and more aerodynamic fore- and hind-limb feathers, so that the lift–drag ratio of these animals progressively became higher, allowing for more efficient gliding. The earliest birds, as exemplified by *Archaeopteryx* and *Confuciusornis*, already possessed fully developed asymmetrical flight feathers [23,40], allowing for longer distance glides, compared with the more basal paravian *Anchiornis*.
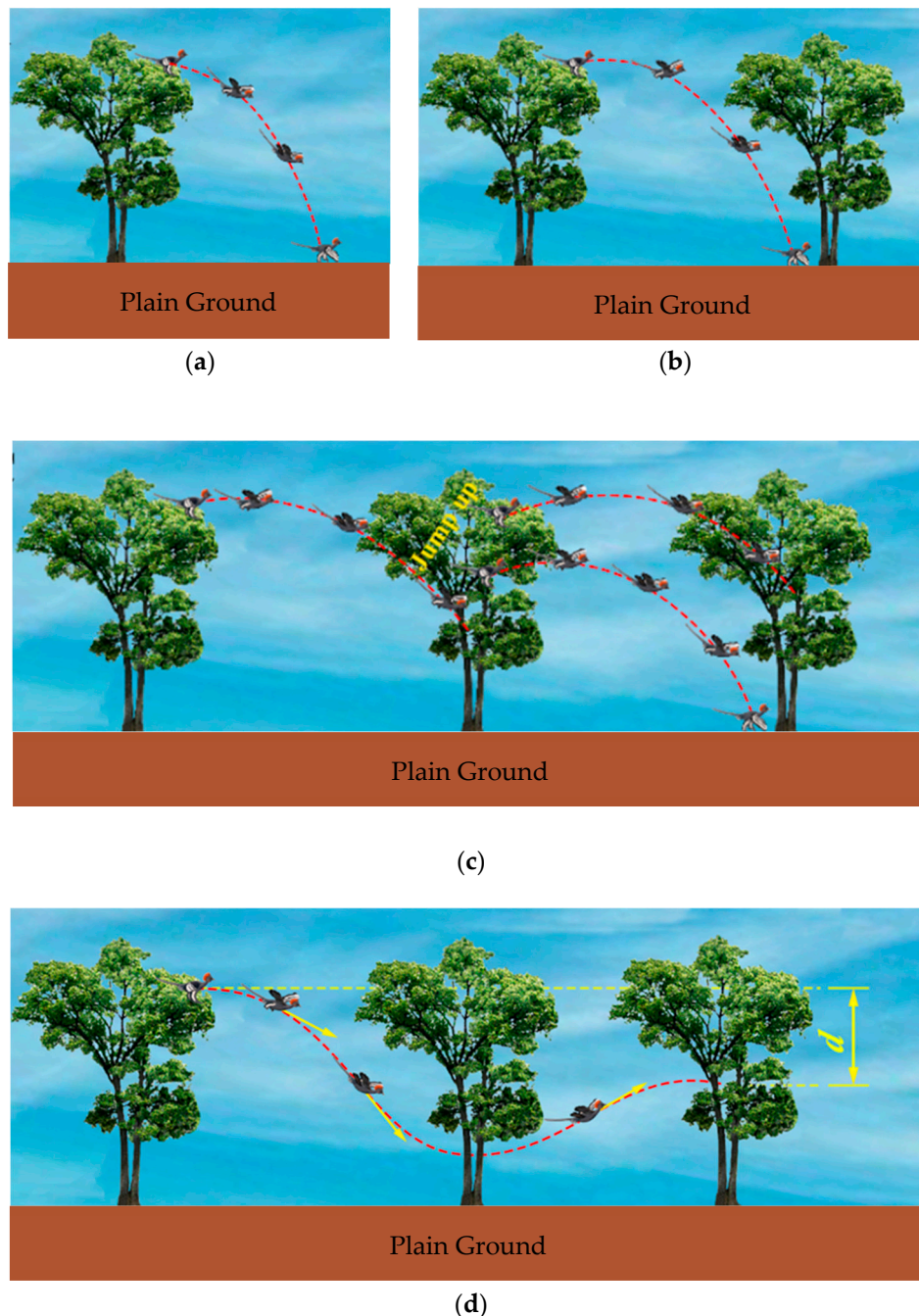

Figure 8. Process of arboreal gliding: (**a**) A theropod parachuting from the branch of a tree to the ground; (**b**) Trying to glide from one tree to another; (**c**) The theropod could glide from the higher position of one tree to the lower position of another; (**d**) The theropod could change its trajectory by adjusting its orientation during gliding so that the resultant force could lift it to a position.

　　　Those early birds could easily parachute from the branch of a tree to the ground or any lower position. Then, later, it could also try to glide from the top branch of one tree to another (Figure 8a,b). Under the action of the potential energy of gravity, the early bird obtained an increasing speed to glide to the lower branch of another tree or changed its trajectory by adjusting its orientation during gliding so that the resultant force could lift it into a position with different heights that were lower than its initial one (Figure 8c). For steady flight conditions in descent when the velocity stays constant, the reciprocal lift–drag ratio should equal the slope of the trajectory. The pes might be used for grasping the branches of the tree when the theropods jumped or walked with the assistance of flapping wings between branches. In this way, they changed their positions in a tree with different heights (Figure 8d). Thus, the early bird could get high enough potential energy before the next glide. It would parachute from the branch of a tree to the ground, as it failed to grasp the branch when it jumped from one branch to another. Practice allowed it to reach another tree by gliding a long enough distance. In this stage, the early birds learned to control their trajectory in gliding [22].

5.3. Stability Control During Gliding

　　　After numerous cycles of gliding with the help of the upslope wind or strong winds in the plains by accident, terrestrial paravians became progressively adapted to a semi-arboreal life, gliding to the trees and then back to the ground. The terrestrial paravians, such as *Anchiornis huxleyi*, could climb the mountain slope from the mountainside after they glided down (Figure S11). Their wings gradually developed ideal shapes and aspect ratios to increase the lift in glide as their feathers became longer and stronger. Because the aerodynamic coefficients are common numerical approximations of complex aerodynamic conditions, which change in flight (e.g., when the angle of attack or effective area of the wings changes), theoretically the non-avian dinosaur could take a continuous glide when the lift, drag, and its self-weight formed a closed vector polygon (Figures S12 (a) and (b)).

　　　As the lift and drag forces are proportional to the aerodynamic coefficients C_L and C_D, the resultant force of lift, drag, and weight should equal zero when the velocity stays constant. The trajectory direction can be therefore expressed by the following:

$$tan\boldsymbol{\theta} = \frac{F_D}{F_L} = \frac{1}{\frac{C_L}{C_D}} \tag{10}$$

where $\boldsymbol{\theta}$ is the subtended angle between the horizontal direction and the airflow and F_L and F_D represent the lift and drag forces resulting from the aerodynamics in gliding.

　　　Equation (10) shows that the slope of the tangent line of any point on the trajectory represents the lift–drag ratio of the aerodynamic coefficients C_L over C_D. The larger the ratio, the more advanced the wings were evolved during the millions of years of the avian ancestors' evolution. During later evolution, early birds learned to change the orientation of their wings to gain higher lifts (Figure S12 (c)). This took place over no more than 15 million years [45,46], which is a very short period relative to the whole history of evolution from the non-avian theropods to the early birds.

　　　We used six rigid bodies of *Anchiornis huxleyi* (Figure S12), including the main body, the four wings, and the tail, to discuss orientation control during gliding. The system dynamics of *Anchiornis huxleyi* can be expressed with Newton–Euler equations. The simplified six-rigid-body dynamics show that the ancestor of the bird could control its pose during gliding. As a matter of fact, the creature could use its flexible body parts to control its pose arbitrarily.

6. Conclusions

　　　Both the cursorial and arboreal hypotheses are insufficient for explaining flight evolution in bird lineage. Here, we presented a biophysical principle to connect both theories and explained how cursorial paravians could reach the top of the trees. Either the upslope winds in the mountain areas in daytime or the strong winds in the plain grounds provided the natural meteorological conditions

for the gliding of avian ancestors from the ground to the trees. In this regard, the gliding between the trees and the ground of paravian theropods might have started long before flight feathers were perfectly aerodynamical.

The results indicate that smaller, feathered paravians were able to generate enough lift to glide down to the trees from the mountain slopes and even perhaps to glide up to high trees in the plain areas in strong air flow. The upslope wind plays an important role in this regard, as can be seen in the plotted figures (provided in this article and the Supplementary Materials), in that as the speed of the wind increases, more lift is produced, and the animal could glide up to a higher position. When the winged paravian parachuted from a high enough position or reached a sufficiently high velocity, it could just use the potential or kinetic energy to travel over a long distance by gliding. Early birds gradually learned to use the meteorological conditions in the mountain and plain areas to get to the trees from the ground and again glide back to the ground. In this stage, the early birds became semi-arboreal.

Trajectories obtained through differential equations can be useful in designing the parameters and control systems for flying robots. The understanding of the origin of flight and its evolution can be beneficial for the design and development of micro air vehicles. The biomimetic mechanism inspired by the evolution of flight can be useful to evaluate an animal's flying apparatus, flying capabilities, control strategy, and stability. The aerodynamic behavior of different extinct animals can be studied in a similar manner in order to fill in the research gaps.

Supplementary Materials: The following are available online at http://www.mdpi.com/2076-3417/9/4/649/s1: Figure S1. Reconstruction of airfoil of *Anchiornis huxleyi*; Figure S2. Interpolated lift coefficient, drag coefficient, and the ratio of lift to drag; Figure S3. Trajectories of *Anchiornis* running at a speed of 6 m/s and θ = 30°; Figure S4. Trajectories of *Anchiornis* running at a speed of 7 m/s and θ = 30°; Figure S5. Trajectories of *Anchiornis* running at a speed of 8 m/s and θ = 30°; Figure S6. Trajectories of *Anchiornis* running at a speed of 6 m/s and θ = 10°; Figure S7. Trajectories of *Anchiornis* running at a speed of 7 m/s and θ = 10°; Figure S8. Trajectories of Anchiornis running at a speed of 8 m/s and θ = 10°; Figure S9. Trajectories of *Anchiornis* running at a speed of 6 m/s and θ = 0°; Figure S10. Trajectories of *Anchiornis* running at a speed of 7 m/s and θ = 0°; Figure S11. Wing-assisted incline running helped *Anchiornis huxleyi* climb the mountain; Figure S12. Forces acting upon a winged theropod during stable gliding flight; and Table S1. Simulation results of the lift and drag coefficients for the thin plate reconstructed in the scale of 1:1 according to the fossil using the ANSYS software.

Author Contributions: All authors have contributed equally to the paper.

Conflicts of Interest: The authors declare no conflicts of interest.

References

1.　Sreetharan, P.S.; Wood, R.J. Passive Aerodynamic Drag Balancing in a Flapping-Wing Robotic Insect. *J. Mech. Des.* **2010**, *132*, 051006. [CrossRef]
2.　Marden, J.H. Maximum Lift Production During Takeoff in Flying Animals. *J. Exp. Btol.* **1987**, *130*, 235–258.
3.　Chin, D.D.; Matloff, L.Y.; Stowers, A.K.; Tucci, E.R.; Lentink, D. Inspiration for wing design: How forelimb specialization enables active flight in modern vertebrates. *J. R. Soc. Interface* **2017**, *14*, 20170240. [CrossRef] [PubMed]
4.　McKellar, R.C.; Chatterton, B.D.E.; Wolfe, A.P.; Currie, P.J. A diverse assemblage of late cretaceous dinosaur and bird feathers from Canadian Amber. *Science* **2011**, *333*, 1619–1622. [CrossRef] [PubMed]
5.　Clarke, J. Feathers before flight. *Science* **2013**, *340*, 690–692. [CrossRef] [PubMed]
6.　Ostrom, J.H. Archaeopteryx: Notice of a "New" Specimen. *Science* **1970**, *170*, 537–538. [CrossRef] [PubMed]
7.　Ostrom, J.H. Bird flight: How did it begin? Did birds begin to fly "from the trees down" or "from the ground up"? Reexamination of Archaeopteryx adds plausibility to an "up from the ground" origin of flight. *Am. Sci.* **1979**, *67*, 46–56. [CrossRef]
8.　Forster, C.A.; Sampson, S.D.; Chiappe, L.M.; Krause, D.W. The theropod ancestry of birds: New evidence from the Late Cretaceous of Madagascar. *Science* **1998**, *279*, 1915–1919. [CrossRef]
9.　Garner, J.P.; Taylor, G.K.; Thomas, A.L.R. On the origins of birds: The sequence of character acquisition in the evolution of avian flight. *Proc. R. Soc. B Biol. Sci.* **1999**, *266*, 1259–1266. [CrossRef]

10. Sereno, P.C. The evolution of dinosaurs. *Science* **1999**, *284*, 2137–2147. [CrossRef]

11. Xu, X.; Zhou, Z.; Wang, X. The smallest known non-avian theropod dinosaur. *Nature* **2000**, *408*, 705–708. [CrossRef] [PubMed]

12. Prum, R.O. Dinosaurs take to the air. *Nature* **2003**, *421*, 323–324. [CrossRef] [PubMed]

13. Paul, G.S. Comment on "Narrow Primary Feather Rachises in Confuciusornis and Archaeopteryx Suggest Poor Flight Ability". *Science* **2010**, *328*, 887–889. [CrossRef] [PubMed]

14. Zheng, X.; Xu, X.; Zhou, Z.; Miao Desui, Z.F. Comment on "Narrow Primary Feather Rachises in Confuciusornis and Archaeopteryx Suggest Poor Flight Ability". *Science* **2010**, *330*, 320. [CrossRef] [PubMed]

15. Nudds, R.L.; Dyke, G.J. Response to Comments on "'Narrow Primary Feather Rachises inConfuciusornis and Archaeopteryx Suggest Poor Flight Ability'". *Science* **2010**, *330*, 320. [CrossRef]

16. Zhang, F.; Zhou, Z. Leg feathers in an early cretaceous bird. *Nature* **2004**, *431*, 925. [CrossRef] [PubMed]

17. Gibbons, A. New Feathered and Dinosaurs Fossil Birds Brings Closer. *Am. Assoc. Adv. Sci.* **1996**, *274*, 720–721. [CrossRef]

18. Dial, K.P. Wing-assisted incline running and the evolution of flight. *Science* **2003**, *299*, 402–404. [CrossRef]

19. Zhang, F.; Zhou, Z. A primitive enantiornithine bird and the origin of feathers. *Science* **2000**, *290*, 1955–1959. [CrossRef]

20. Zelenitsky, D.K.; Therrien, F.; Erickson, G.M.; DeBuhr, C.L.; Kobayashi, Y.; Eberth, D.A.; Hadfield, F. Feathered non-avian dinosaurs from North America provide insight into wing origins. *Science* **2012**, *338*, 510–514. [CrossRef]

21. Xu, X.; Zhou, Z.; Wang, X.; Kuang, X.; Zhang, F.; Du, X. Four-winged dinosaurs from China. *Nature* **2003**, *421*, 335–340. [CrossRef] [PubMed]

22. Chatterjee, S.; Templin, R.J. The flight of Archaeopteryx. *Naturwissenschaften* **2003**, *90*, 27–32. [CrossRef] [PubMed]

23. Zhou, Z. The origin and early evolution of birds: Discoveries, disputes, and perspectives from fossil evidence. *Naturwissenschaften* **2004**, *91*, 455–471. [CrossRef] [PubMed]

24. Feduccia, A. Evidence from Claw Geometry Indicating Arboreal Habits of Archaeopteryx. *Science* **1993**, *259*, 790–793. [CrossRef] [PubMed]

25. Zheng, X.; Zhou, Z.; Wang, X.; Zhang, F.; Zhang, X.; Wang, Y.; Wei, G.; Wang, S.; Xu, X. Hind wings in basal birds and the evolution of leg feathers. *Science* **2013**, *339*, 1309–1312. [CrossRef] [PubMed]

26. Ruben, J.A. Reptilian physiology and the flight capacity of Archaeopteryx. *Evolution* **1991**, *45*, 1–17. [CrossRef] [PubMed]

27. Speakman, J. Flight capabilities of Archaeopteryx. *Int. J. Org. Evol.* **1993**, *47*, 336–340. [CrossRef]

28. Dong, S.W.; Zhang, Y.Q.; Long, C.X.; Yang, Z.Y.; Ji, Q.; Wang, T.; Hu, J.M.; Chen, X.H. Jurassic tectonic revolution in China and new interpretation of the "Yanshan Movement.". *Acta Geol. Sin. Ed.* **2008**. [CrossRef]

29. Yongdong, W.; Ken' ichi, S.; Wu, Z.; Shaolin, Z. Biodiversity and palaeoclimate of the Middle Jurassic floras from the Tiaojishan Formation in western Liaoning, China. *Prog. Nat. Sci.* **2006**, *16*, 222–230. [CrossRef]

30. Sullivan, C.; Wang, Y.; Hone, D.W.E.; Wang, Y.; Xu, X.; Zhang, F. The vertebrates of the Jurassic Daohugou Biota of northeastern China. *J. Vertebr. Paleontol.* **2014**. [CrossRef]

31. Vergeiner, I.; Dreiseitl, E. Valley winds and slope winds—Observations and elementary thoughts. *Meteorol. Atmos. Phys.* **1987**, *36*, 264–286. [CrossRef]

32. Kleissl, J.; Honrath, R.E.; Dziobak, M.P.; Tanner, D.; Val Martín, M.; Owen, R.C.; Helmig, D. Occurrence of upslope flows at the Pico mountaintop observatory: A case study of orographic flows on a small, volcanic island. *J. Geophys. Res. Atmos.* **2007**, *112*, 1–16. [CrossRef]

33. Whiteman, C.D.; Doran, J.C. The relationship between overlying synoptic-scale flows and winds within a valley. *J. Appl. Meteorol.* **1993**, *32*, 1669–1682. [CrossRef]

34. Whiteman, C.D. *Mountain Meteorology: Fundamentals and Applications*; Oxford University Press: Oxford, UK, 2000; ISBN 0-19-513271-8.

35. Longrich, N.R.; Vinther, J.; Meng, Q.; Li, Q.; Russell, A.P. Primitive wing feather arrangement in Archaeopteryx lithographica and Anchiornis huxleyi. *Curr. Biol.* **2012**, *22*, 2262–2267. [CrossRef] [PubMed]

36. Hu, D.; Hou, L.; Zhang, L.; Xu, X. A pre-Archaeopteryx troodontid theropod from China with long feathers on the metatarsus. *Nature* **2009**, *461*, 640–643. [CrossRef] [PubMed]

37. Zhang, F.; Zhou, Z.; Xu, X.; Wang, X.; Sullivan, C. A bizarre Jurassic maniraptoran from China with elongate ribbon-like feathers. *Nature* **2008**, *455*, 1105–1108. [CrossRef] [PubMed]

38. Kurochkin, E.N.; Dyke, G.J.; Saveliev, S.V.; Pervushov, E.M.; Popov, E.V. A fossil brain from the Cretaceous of European Russia and avian sensory evolution. *Biol. Lett.* **2007**, *3*, 309–313. [CrossRef]

39. Xu, X.; Zhao, Q.; Norell, M.; Sullivan, C.; Hone, D.; Erickson, G.; Wang, X.; Han, F.; Guo, Y. A new feathered maniraptoran dinosaur fossil that fills a morphological gap in avian origin. *Chin. Sci. Bull.* **2009**, *54*, 430–435. [CrossRef]

40. Nudds, R.L.; Dyke, G.J. Narrow primary feather rachises in Confuciusornis and Archaeopteryx suggest poor flight ability. *Science* **2010**, *328*, 887–889. [CrossRef]

41. Carney, R.M.; Vinther, J.; Shawkey, M.D.; D'Alba, L.; Ackermann, J. New evidence on the colour and nature of the isolated Archaeopteryx feather. *Nature Commun.* **2012**, *3*, 637. [CrossRef]

42. Xu, X.; Norell, M.A. Non-avian dinosaur fossils from the Lower Cretaceous Jehol Group of western Liaoning, China. *Geol. J.* **2006**, *41*, 419–437. [CrossRef]

43. O'Connor, J.; Zhou, Z.; Xu, X. Additional specimen of Microraptor provides unique evidence of dinosaurs preying on birds. *Proc. Natl. Acad. Sci. USA* **2011**, *108*, 19662–19665. [CrossRef] [PubMed]

44. Li, Q.; Gao, K.; Vinther, J.; Shawkey, M.D.; Clarke, J.; D'alba, L.; Meng, Q.; Briggps, D.E.G.; Prum, R.O. Plumage Color Patterns of an. *Science* **2010**, *327*, 1369–1372. [CrossRef] [PubMed]

45. Sereno, P.C.; Chenggang, R. Early Evolution of Avian Flight and Perching: New Evidence from the Lower Cretaceous of China. *Science* **2014**, *255*, 845–848. [CrossRef] [PubMed]

46. Padian, K.; Chiappe, L.M. The origin and early evolution of birds. *Biol. Rev.* **1998**. [CrossRef]